SCIENCE CHINA
Information Sciences

• RESEARCH PAPER •

March 2026, Vol. 69, Iss. 3, 132401:1–132401:8
https://doi.org/10.1007/s11432-025-4528-6

# Artificial intelligence—assisted pump-locked random lasers

Junhua TONG[1], Xiaoyu SHI[2], Zhiyang XU[2], Naeem IQBAL[2], Kun GE[2] & Tianrui ZHAI[2*]

[1]*College of Mathematics and Physics, Beijing University of Chemical Technology, Beijing 100029, China*
[2]*School of Physics and Optoelectronic Engineering, Beijing University of Technology, Beijing 100124, China*

Received 16 April 2025/Revised 30 May 2025/Accepted 25 July 2025/Published online 4 January 2026

**Abstract** Random lasing in complex disordered systems demonstrates lasing efficiency across multiple localized modes. Accurate control of these modes can enable random lasers to function as fast-switching multifunctional light sources. In this work, an unpredictable random laser was prepared, and artificial intelligence technology was used for taming the lasing action. Lasing modes were precisely controlled by programming the spatial shape of the pump profile. Genetic algorithms were introduced, allowing any mode within the complex system to be extracted by setting a target value associated with that mode. Based on experimental results, the interaction model of pump cells with lasing modes was locked. This work advances programmable random lasers, enhancing their potential for practical applications in signal processing, spectral sensing, communication, and optical computing.

**Keywords** random lasers, artificial intelligence, genetic algorithms, mode selection, pump-locked

**Citation** Tong J H, Shi X Y, Xu Z Y, et al. Artificial intelligence—assisted pump-locked random lasers. Sci China Inf Sci, 2026, 69(3): 132401, https://doi.org/10.1007/s11432-025-4528-6

## 1 Introduction

Random lasers, characterized by low spatial coherence [1, 2], multimodal operation [3], intensity fluctuations [4], and diverse physical phenomena [5], exhibit potential for applications in speckle-free imaging [6, 7], biosensing [8], super-resolution spectroscopy [9], and cross-disciplinary research platforms [10]. However, limited controllability over lasing modes, such as emission frequency, threshold, and direction, restricts the application of random lasers in spectral sensing, signal processing, optical computing, and communication. Directional random lasing has been achieved by incorporating directional components, such as optical microcavities (fiber, waveguide, distributed Bragg reflectors, and spherical microcavities) [11–14]. Control over random lasing frequency and threshold is mainly exerted by manipulating gain materials and scattering paths [15–17]. However, these methods typically yield only an overall shift in lasing frequency [18]. Manually extracting specific modes from the numerous lasing modes is highly challenging due to strong intermode correlations in complex disordered systems.

With the rapid advancement of artificial intelligence (AI) technology, its interdisciplinary integration has expanded scientific research boundaries. Notably, optics, as a foundational research field, is at the forefront of this integration. Currently, AI and optics converge primarily in two areas: empowering AI with optics, where photons replace traditional electronics for more efficient AI computing [19,20], and empowering optics with AI, where intelligent algorithms are used to accelerate the design and optimization of optical devices [21]. Deep learning models, such as multilayer perceptron neural networks, enable the rapid design and characterization of microstructures and nanostructures [22]. In summary, AI algorithms now enable researchers to bypass inefficient processes, enabling everything from theoretical model integration to complex simulations of optical phenomena and intelligent light field analysis.

Theoretical and experimental evidence indicates that shaping the pump profile can precisely extract specific modes from random lasers [23–28]. Using genetic algorithms (GAs) in AI, we can now demonstrate the mode extraction process from an experimental perspective. Sebbah's research group first reported this process in predesigned structured systems, such as one-dimensional random systems [29–31]. Saxena et al. [32] realized spectral control in a network laser via selective pumping by solving the network laser using steady-state ab initio laser theory. Nonetheless, in a complex random structure lacking a predefined design, it remains challenging to efficiently extract specific modes and lock their corresponding pump patterns. In this work, we successfully extracted specific

* Corresponding author (email: trzhai@bjut.edu.cn)

© Science China Press 2026 

lasing modes within a disordered system using GAs. Notably, the relationship between pump cells and lasing modes can be established by comparing the pump profiles of the corresponding modes. This approach enables effective prediction of optical paths for random lasing generation, providing a means to determine the generation principles of random lasing action and advancing the performance customization of random lasers.

## 2 Design principles

Random lasing is boosted by multiple and recurrent scattering of light in a gain medium. The pump profile determines the stimulated region within the random system, influencing optical scattering feedback and gain paths, which, in turn, control the lasing modes. Thus, the spatial distribution of the emitted laser light from the random laser exhibits variations when the spatial distribution of the pump light changes. However, the spatial distribution of modes is random, which is a key feature that distinguishes random lasers from conventional ones [33]. That is to say, the change in the pump light spatial distribution cannot cause the focusing of a certain mode. A disordered membrane was fabricated using a simple spin coating method (Section 5 and Figure S1). Typically, a digital micromirror device (DMD) is used to shape pump profiles. However, manually importing pump patterns makes it challenging to extract specific modes from the many lasing modes. Thus, intelligent methods are required. Figures 1(a) and (b) illustrate the principles of mode selection in random lasers using our intelligent control system. The core of the intelligent control system is a self-developed software comprising a GA, a DMD control program, and a spectral acquisition program (Figure S2). GAs are effective methods for global target searching [34]. Based on a predefined target mode ($\lambda_t$) and the initial spectral data under a uniform pump profile, the GA optimization program infers the required pump profile for the next cycle. By accessing the DMD program interface, the DMD control program converts the 2D pump profile image data into 1D data and transmits them to the DMD. Based on image grayscale, the program autonomously controls the DMD reflectors to adjust the pump light, thereby controlling the pump pattern. The spectral acquisition program, based on the preset parameters, acquires random lasing spectra excited by the pump pattern through spectrometer control. Through iterative optimization, the target modes are obtained (Figure 1(c)). The corresponding pump patterns for the selected modes can then be locked and analyzed. This enables the prediction of possible optical paths for the random lasing modes.

## 3 Results and discussion

As well-known intelligent algorithms, GAs include key components: population, fitness selection, and evolutionary operators, as shown in Figure 2(a). These evolutionary operators include selection, crossover, and mutation. A population of possible solutions is employed to search the solution space. Each solution is encoded as a character string, which is referred to as a genome. In each iteration, the fitness values of genomes are evaluated, and those with higher fitness have an increased probability of survival. The surviving genomes combine to form "child" genomes through a process called crossover. In addition, genomes may undergo mutation. Finally, a new iteration is formed by recombining and replacing the initial population. This process is repeated to yield stronger solutions over successive iterations until the target solution is found.

In our work, the population comprises image data representing possible pump profiles. The fitness function assigns a value to each genome in the population. The fitness function is defined as

$$f\left(\lambda_t\right)=\frac{\operatorname{Max}\left\{I_{\lambda_{s1}}, I_{\lambda_{s2}}, \ldots, I_{\lambda_{sn}}\right\}}{\operatorname{Min}\left\{I_{\lambda_{t1}}, I_{\lambda_{t2}}, \ldots, I_{\lambda_{tm}}\right\}},$$

where $\lambda_t$ and $\lambda_s$ represent the modes to be selected and suppressed, respectively, $m$ is the number of target modes ($m \geqslant 1$), and $n$ is the number of suppressed modes ($n \geqslant 0$). Max denotes the maximum peak intensity among the suppressed modes, while Min denotes the minimum peak intensity among the target modes. Thus, a smaller $f(\lambda_t)$ value in the optimization process indicates greater dominance of the target modes. The target modes are selected when $f(\lambda_t)$ converges to an ideal value ($\leqslant 0.5$), ensuring that the side-mode suppression ratio (SMSR) is greater than 10 dB. Figure 2(b) shows the evolution of $f(\lambda_t)$ across iteration cycles for selecting a specific mode. The value converges to approximately 0.21. The inset displays the optimization process of the pump profiles. When the sample is excited by a uniform pump profile, random lasing with multiple modes is observed, as shown in the upper panel in Figure 2(c). In contrast, when the sample is excited by an optimized pump profile, the target mode is accurately selected, and the other modes are effectively suppressed, as shown in the lower panel in Figure 2(c). The SMSR reaches 14.8 dB in the single-mode spectra. In the mode selection process, the sample was pumped with energy that is lower than its damage threshold, which can prevent photobleaching.

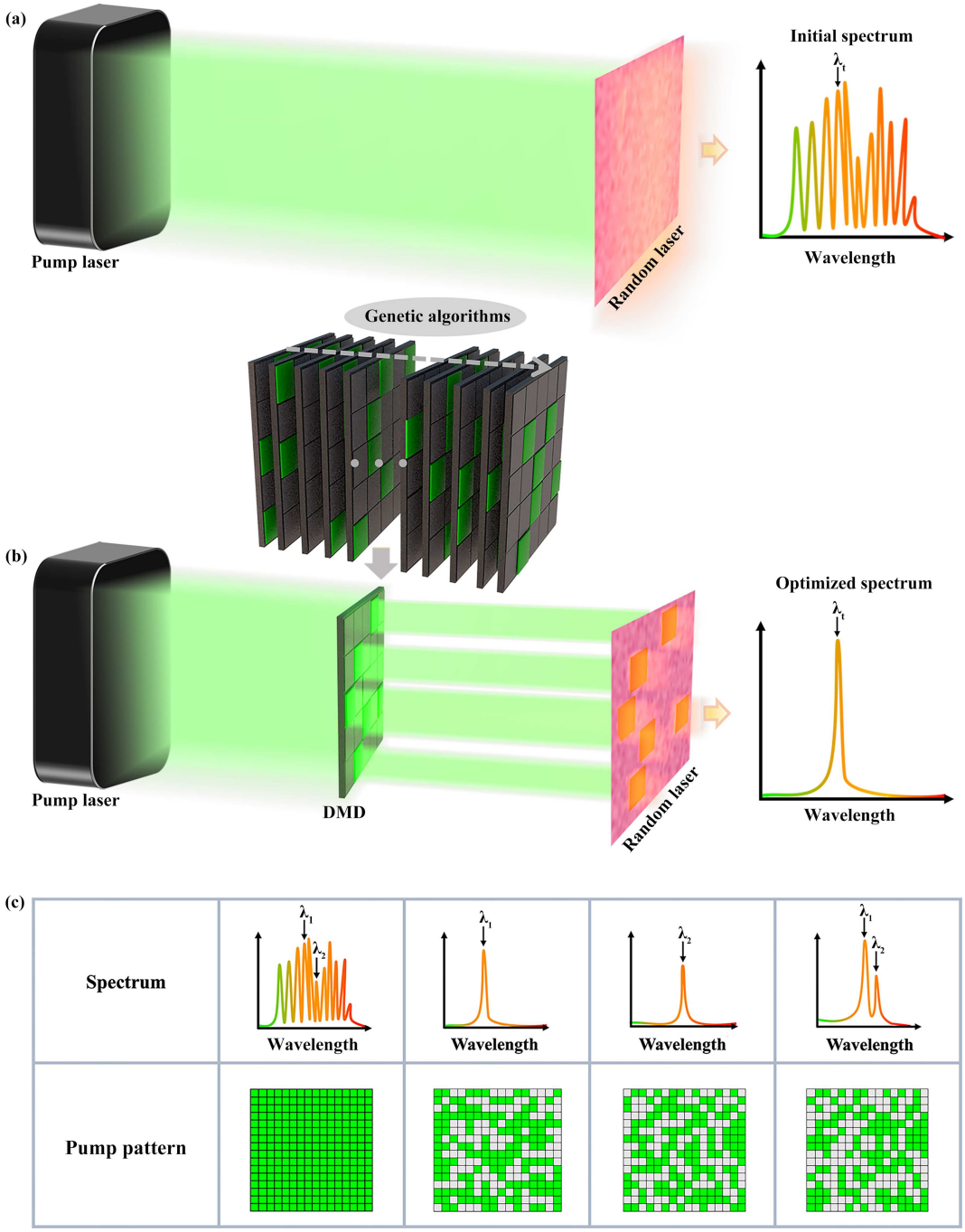


**Figure 1** (Color online) Principles of mode selection in random lasers using an intelligent control system. (a) Diagram of pump control with a uniform pump profile to obtain the initial spectrum; (b) diagram of intelligent pump control by the digital micromirror device (DMD) to obtain the target mode, which is represented by $\lambda_t$; (c) selected random lasing modes with their corresponding pump patterns.

Once the pump profile is determined, the target mode can be accurately selected. As a result, the emission characteristics of a single-mode operation versus a multimode operation were explored in this work, as shown in Figures 2(c) and (d). Random lasing with multiple modes was obtained by exciting the sample with a uniform pump profile, as shown in the upper panel in Figure 2(c). As the pump power density increases, the emission spectrum evolves from a typical fluorescent spectrum to a multimode random lasing spectrum. To verify the effect of mode selection, the optimized pump profile was applied to excite the sample. The lower panel in Figure 2(c) shows the emission spectra at different pump power densities, yielding a stable single-mode random lasing with a higher intensity. Furthermore, the threshold behavior for a specific mode, pumped by the uniform and optimized profiles, is shown in Figure 2(d). The threshold at 589 nm with optimized pumping is approximately 0.55 MW/cm$^2$, which

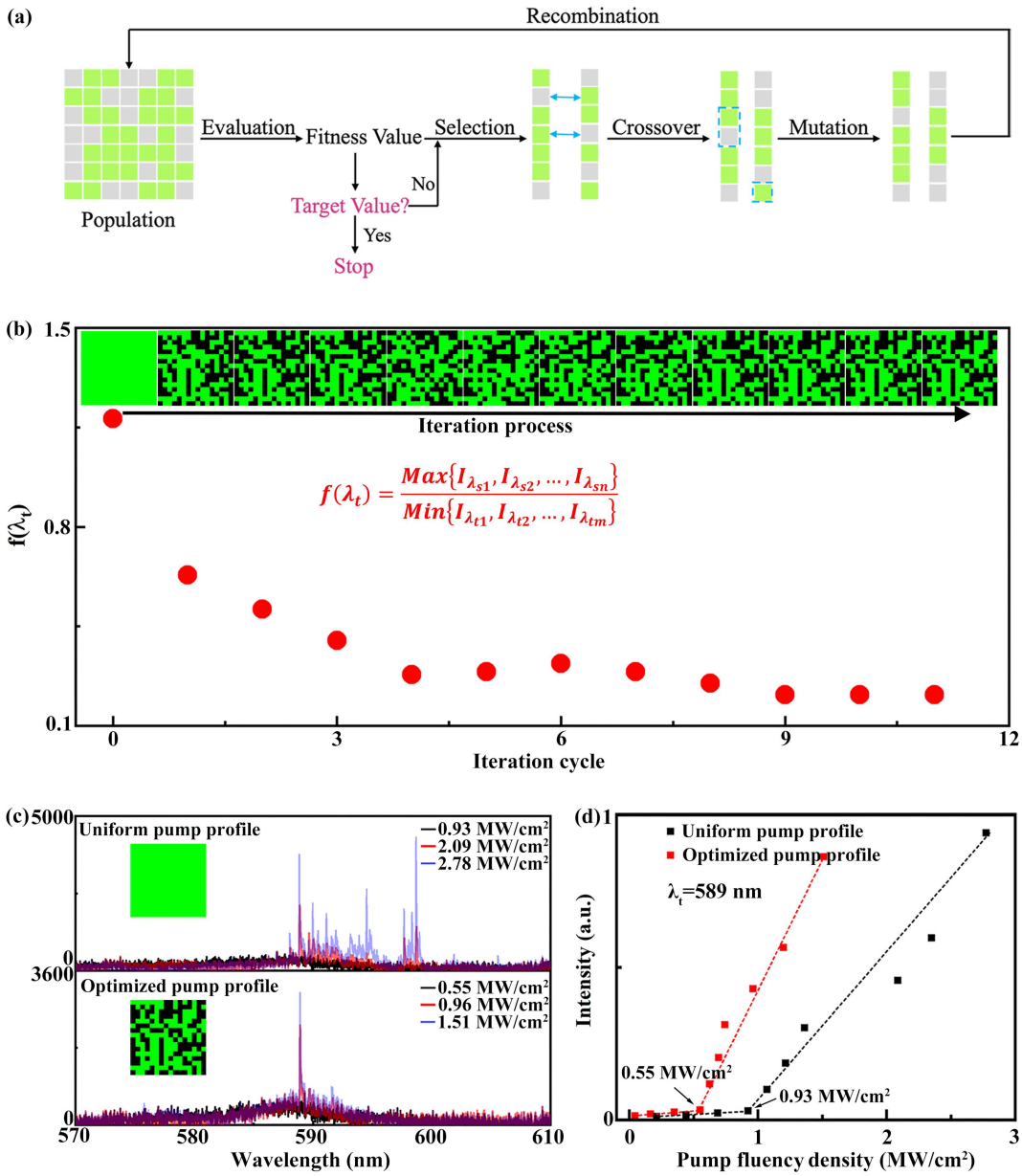


**Figure 2** (Color online) Single-mode selection operation. (a) Genetic algorithms (GAs) applied to pump pattern optimization within our self-developed software. (b) Convergence of the optimization process: score evolution across iteration cycles for single-mode optimization. Here, 50 score values are selected per iteration cycle, and the pump profile with the optimal score is used for the subsequent cycle. Gray values are set to either 0 (black) or 255 (green). (c) Emission spectra excited by a uniform pump profile (upper panel) and an optimized pump profile (lower panel) under varying pump power densities. (d) Emission intensity of random lasing as a function of pump fluence for the uniform and optimized pump profiles. The corresponding uniform and optimized pump profiles, as displayed on the DMD, are shown in the inset in (c).

is nearly half of that with uniform pumping. Overall, these results demonstrate that our proposed intelligent control system not only accurately extracts modes but also maintains a stable lasing emission under the optimized pump profile. In addition, we studied the influence of fiber probe position on the lasing modes. Once the pump profile was fixed, the emission spectra were collected at a fixed pump energy density (1.51 MW/cm$^2$) and various observation angles ($\theta$ = 60°, 30°, 0°, −30°, −60°; $\theta$ represents the angle formed by the normal vector of the sample and the direction of observation), as shown in Figure S3. The results indicate that the lasing characteristics (wavelength, linewidth, and intensity) almost did not change, which is a distinct indication of the occurrence of random laser activity [35]. That is to say, the lasing modes are independent of detection position.

To further test the mode extraction capability of our proposed intelligent control system, we attempted to extract arbitrary single modes and multimodes, as shown in Figure 3. When the sample is pumped by a uniform profile at a higher pump power density, a random lasing spectrum with multiple modes is obtained, as shown in Figure 3(a).

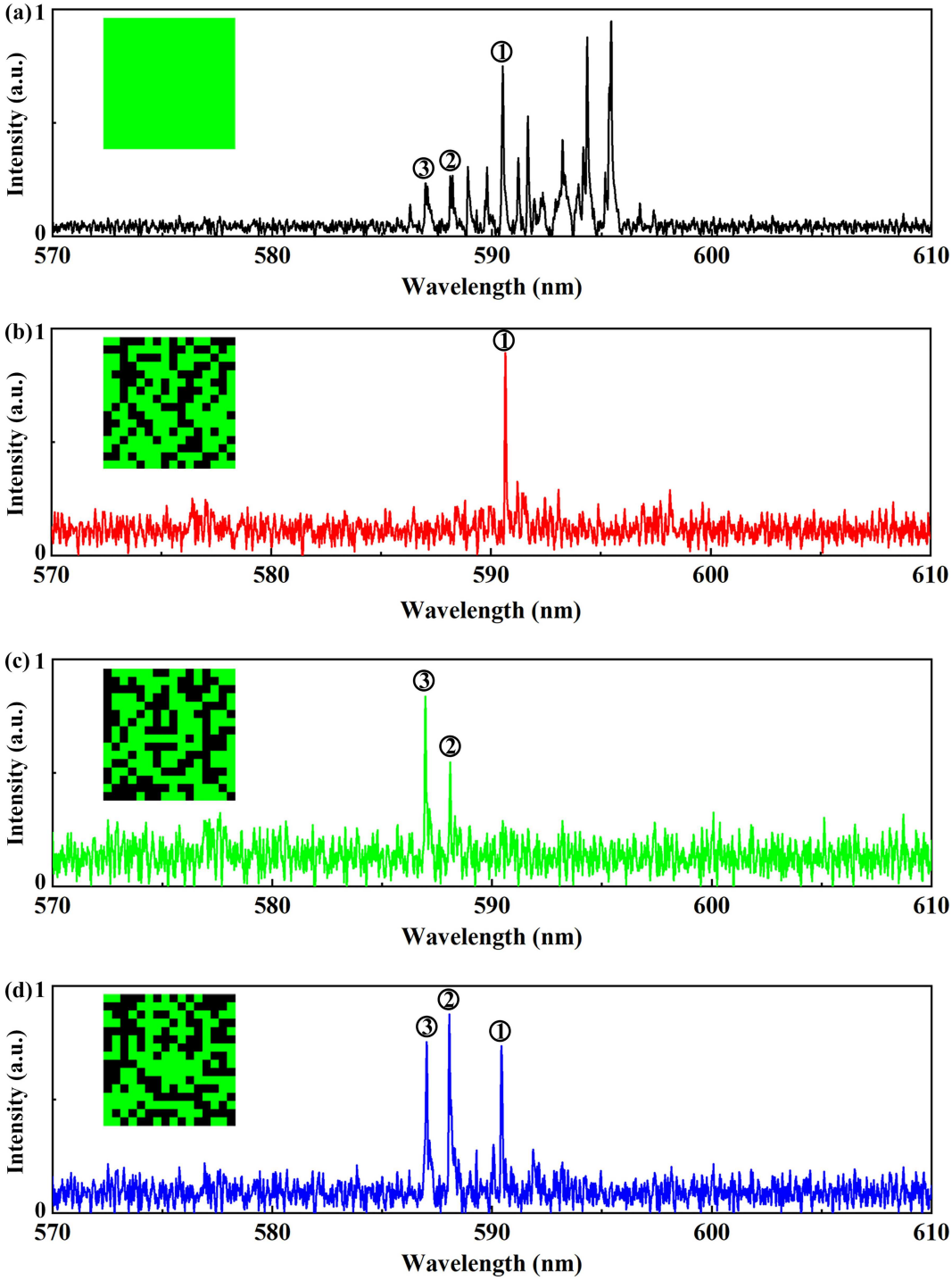


**Figure 3** (Color online) Extraction of arbitrary single modes and multimodes. (a) Random lasing spectrum with multiple modes excited by a uniform pump profile. (b) Random lasing spectrum with a single mode at 590.5 nm. (c) Random lasing spectrum with two modes at 587.0 and 588.1 nm. (d) Random lasing spectrum with three modes at 587.0, 588.1, and 590.5 nm. The insets show the corresponding pump profiles. The symbols ①, ②, and ③ indicate the modes at 590.5, 588.1, and 587.0 nm, respectively.

Keeping all other conditions unchanged, we set a single mode (590.5 nm), two modes (587.0 and 588.1 nm), and three modes (587.0, 588.1, and 590.5 nm) in the original spectrum as the target modes. We adjusted the search parameters in the GA optimization program to control the pump pattern in the DMD until the target modes were obtained. In addition, the modes at 587.0 and 588.1 nm can be individually extracted effectively. We have added the optimized results in Figure S4. Notably, according to the omnidirectional emission of the random lasers, the collected emission spectra are almost independent of angle. In addition, the size of the pumped area is comparable

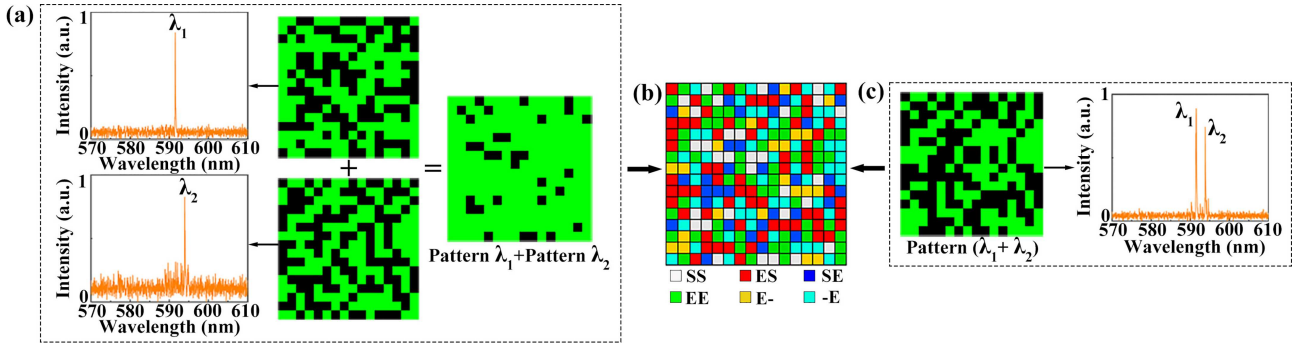


**Figure 4** (Color online) Analysis of the pump-locked random lasers. Random lasing spectra and corresponding pump patterns for (a) single modes at 591.5 nm ($\lambda_1$) and 594.0 nm ($\lambda_2$) and (c) a dual mode ($\lambda_1$ and $\lambda_2$). (b) Effect of pump cells on the selection of $\lambda_1$ and $\lambda_2$. Here, "S" and "E" indicate suppression and enhancement, respectively. The symbol "-" represents no effect on mode selection. For example, "ES" indicates that red pump cells enhance $\lambda_1$ while suppressing $\lambda_2$ simultaneously.

to the entrance aperture of the fiber-optic spectrometer. Thus, the spectra include all the emitted lasing modes that can be collected. These results indicate that any target mode within a complex disordered system can be accurately extracted using our proposed intelligent control system, even the adjacent modes and modes that are at a competitive disadvantage, such as those at 587.0 and 588.1 nm.

For random lasers, the pump pattern determines the excited region of the sample, affecting the optical paths for lasing generation. Thus, locking the role of each pump cell in the lasing mode provides an effective method for exploring optical feedback paths. In our work, two modes ($\lambda_1$ and $\lambda_2$) were selected individually or simultaneously for analysis, as shown in Figure 4. A video recording of the optimization process is provided in the supporting information. The spectra and corresponding pump patterns for single modes $\lambda_1$ and $\lambda_2$ are shown in Figure 4(a). In contrast, Figure 4(c) shows the spectrum and corresponding pump pattern for a dual mode ($\lambda_1$ and $\lambda_2$). For comparison, the linear superposition of the pump patterns for $\lambda_1$ and $\lambda_2$ was also calculated, as shown in Figure 4(a), where the number of pump cells is significantly higher and can cover the combined pattern ($\lambda_1 + \lambda_2$) in Figure 4(c). Based on these results, we analyzed the effect of pump cells on $\lambda_1$ and $\lambda_2$ selection, as shown in Figure 4(b). The gray cells (SS) simultaneously suppress $\lambda_1$ and $\lambda_2$, while the green cells (EE) simultaneously enhance $\lambda_1$ and $\lambda_2$. The red cells (ES) enhance $\lambda_1$ but suppress $\lambda_2$, while the blue cells (SE) suppress $\lambda_1$ but enhance $\lambda_2$. The orange cells (E-) enhance $\lambda_1$ with no effect on $\lambda_2$, while the cyan cells (-E) enhance $\lambda_2$ with no effect on $\lambda_1$. That is to say, a pump-locked random laser for a certain mode is achieved for the first time.

The coupling relationship between modes can be predicted based on the locked pump cells and mode intensities. When extracting single modes $\lambda_1$ and $\lambda_2$ in turn, the number of illuminated cells is 144 and 136, respectively, as shown in Figure 4(a). Clearly, $\lambda_1$ is easier to extract with a strong intensity, indicating that it has relatively dominant optical feedback paths. $\lambda_2$ is more difficult to extract alone from tens of modes in the initial spectrum, indicating weaker competitiveness and considerable overlap in the optical feedback paths with competing modes. When extracting the two modes simultaneously, the number of illuminated cells is up to 129, as shown in Figure 4(c). By comparing Figure 4(c) with Figure 4(a), it is easier to extract the two modes than any single one with a higher intensity, especially $\lambda_2$. All these results indicate that there is an overlap between their optical feedback paths, which has more influence on $\lambda_2$. This work thus provides an effective method for analyzing the coupling relationships between random lasing modes.

## 4 Conclusion

A powerful tool for mode selection in an unpredictable random system is first demonstrated. By building an intelligent pump control system based on GAs, any expected modes can be extracted accurately and efficiently, while the effect of pump cells on specific modes can be locked. Based on the locked pump cells and corresponding mode intensity, the coupling relationship between modes can be deduced. This work breaks through the barrier of quantitatively controlling modes in complex disordered systems and can guide the reverse design of photonic devices.

## 5 Experimental section

Sample preparation. In the sample fabrication, we tried to realize an ultralowthreshold random laser by optimizing the sample parameters. The disordered system was a polymer film fabricated using a dye-doped Poly(methyl methacrylate) (PMMA) polymer with scattering nanoparticles. In this work, the typical laser dye RhB was used as the gain material, while Au nanorods (NRs) with diameters and lengths of approximately 25 and 50 nm, respectively, acted as scatterers. The Au NRs provide coherent feedback in the polymer film and enhance the RhB emission due to localized surface plasmon resonance in the local electric field. The fabrication process is illustrated in Figure S1. First, the Au NRs (0.02 mg/mL) were spin-coated onto a flexible PET substrate at 1800 r/min for 40 s. Second, RhB (6 mg/mL) and PMMA (200 mg/mL) were mixed at a 1:1 volume ratio and magnetically stirred for 20 min. Then, the mixture was spin-coated onto the Au NR layer at 1800 r/min for 40 s. Next, the structure was heated at 70°C for 20 min to achieve solidification. Finally, a uniform film with a size of 5 cm × 5 cm was obtained, which can be cut into smaller samples. Dichloromethane was used as the solvent in all the steps.

Intelligent control system. The core of the intelligent control system is a self-developed software comprising a GA optimization program, a DMD control program, and a spectral acquisition program. The model-view-controller architecture was used in our self-developed software, which can separate different parts of an application program (the main code in the PDF version in the supporting information), improving the system's maintainability, expandability, testability, and flexibility. The modular design lays a good foundation for the expansion of the software functions, including debugging, optimizing, and replacing the algorithm. The software interface mainly contains parts of the spectrum display, parameter setting, regulation, and control. The spectrum display area displays the current spectrum data. The parameter setting area for spectrum acquisition can set the smoothing points of the spectrometer, the spectrum acquisition time, and the spectrum average number. The parameter setting area for the spectrum frequency can set the frequency that needs to be enhanced and suppressed. The regulation and control areas are used to start or stop the control function. To extract the target mode more efficiently, some detailed parameter settings were conducted. The emission frequency range of the sample under uniform pumping was first determined, which can be used to precisely set the spectral optimization range. The optimized frequency range of a target mode was set equivalent to its linewidth. It can prevent target mode loss caused by the spectral fluctuation and eliminate the interference of adjacent modes. In addition, a constant was added to the molecular term on the numerator of the fitness function $f(\lambda_t)$, enhancing the SMSR. The experimental results indicate that these methods are efficient for mode selection.

Optical measurement. The diagram of the test setup based on the intelligent control system is illustrated in Figure S2. A doubled Q-switched Nd:YAG laser (532 nm, 5–7 ns, 10 Hz) was employed as the pump source. Lenses 1 and 2 were used for expanding and collimating the pump beam, respectively. The DMD (ViALUX: V-7000) was used to shape the pump profile based on the feedback of the grayscale of the image. The maximum array switching rate of the DMD was 22727 Hz (1 bit B/W). In addition, the image grayscale can be modulated by controlling the opening time of a pixel through adjustment of the time duty ratio. The array switching rate of a 6 bit (8 bit) gray image was 1091 Hz (290 Hz). In our work, the grayscale modulation of the DMD is inconvenient for the real-time optimization of the pump profile. The modulated pump light is reflected to lens 3. Lens 3 was used to adjust the size of the pump profile. In this work, the size of the pumped area was 0.01 $mm^2$ (0.1 mm × 0.1 mm), which is comparable to the entrance aperture of the fiber-optic spectrometer. Thus, the scale of a single random laser depends on the size of the light spot pumped on the sample. The pump spot was set to 256 (16 × 16) optimization units, indicating that each optimization unit was 6.25 μm × 6.25 μm. The modulated pump pattern was vertically incident on the sample. The emission light was collected at an observation angle $\theta$ ($\theta \approx 30°$) using an optical fiber spectrometer (Ocean Optics HR4000) with a spectral resolution of 0.02 nm. The pump power was controlled by the pump voltage. The pump source, DMD, and high-resolution spectrometer were linked using the self-developed software.

**Acknowledgements** This work was financially supported by National Natural Science Foundation of China (Grant Nos. 62375007, 62405012) and Beijing Natural Science Foundation (Grant Nos. 1232024, 4244102).

**Supporting information** Figures S1–S4. The supporting information is available online at info.scichina.com and link.springer.com. The supporting materials are published as submitted, without typesetting or editing. The responsibility for scientific accuracy and content remains entirely with the authors.

**References**

1 Cao H, Chriki R, Bittner S, et al. Complex lasers with controllable coherence. Nat Rev Phys, 2019, 1: 156–168
2 Ni L Q, Qi Y F, Bao X Y, et al. Temporal-spectral correlation dynamics of Raman random fiber laser. Sci China Inf Sci, 2025, 68: 140404
3 Sapienza R. Determining random lasing action. Nat Rev Phys, 2019, 1: 690–695
4 Sapienza R. Controlling random lasing action. Nat Phys, 2022, 18: 976–979

5 Du W, Hu L, Xia J, et al. Observation of the photonic Hall effect and photonic magnetoresistance in random lasers. Nat Commun, 2024, 15: 4589
6 Redding B, Choma M A, Cao H. Speckle-free laser imaging using random laser illumination. Nat Photon, 2012, 6: 355–359
7 Lin J Z, Guo D, Zhai T R. Lead-free metal halide scintillator materials for imaging applications. Sci China Inf Sci, 2024, 67: 181401
8 Xu Z, Hong Q, Ge K, et al. Random lasing from label-free living cells for rapid cytometry of apoptosis. Nano Lett, 2022, 22: 172–178
9 Boschetti A, Taschin A, Bartolini P, et al. Spectral super-resolution spectroscopy using a random laser. Nat Photonics, 2020, 14: 177–182
10 Ghofraniha N, Viola I, Di Maria F, et al. Experimental evidence of replica symmetry breaking in random lasers. Nat Commun, 2015, 6: 6058
11 Shi X Y, Shen K Y, Bian Y X, et al. Programmable complex pumping field induced color-on-demand random lasing in fiber-integrated microbelts for speckle free imaging. Sci China Inf Sci, 2023, 66: 222401
12 Zhai T, Zhang X, Pang Z, et al. Random laser based on waveguided plasmonic gain channels. Nano Lett, 2011, 11: 4295–4298
13 Liu Y, Yang W, Xiao S, et al. Surface-emitting perovskite random lasers for speckle-free imaging. ACS Nano, 2019, 13: 10653–10661
14 Lee K R, Ma H J, Rotermund F, et al. Non-resonant power-efficient directional Nd:YAG ceramic laser using a scattering cavity. Nat Commun, 2021, 12: 8
15 Adl H P, Sánchez-Díaz J, Vescio G, et al. Tailoring single-mode random lasing of tin halide perovskites integrated in a vertical cavity. Adv Mater, 2024, 36: 2313252
16 Li X, Wang Y, Sun H, et al. Amino-mediated anchoring perovskite quantum dots for stable and low-threshold random lasing. Adv Mater, 2017, 29: 1701185
17 Bian Y, Xue H, Wang Z. Programmable random lasing pulses based on waveguide-assisted random scattering feedback. Laser Photonics Rev, 2021, 15: 2000506
18 Gomes A S L, Moura A L, de Araújo C B, et al. Recent advances and applications of random lasers and random fiber lasers. Prog Quantum Electron, 2021, 78: 100343
19 Wetzstein G, Ozcan A, Gigan S, et al. Inference in artificial intelligence with deep optics and photonics. Nature, 2020, 588: 39–47
20 Lin X, Rivenson Y, Yardimci N T, et al. All-optical machine learning using diffractive deep neural networks. Science, 2018, 361: 1004–1008
21 Wang N, Yan W, Qu Y, et al. Intelligent designs in nanophotonics: from optimization towards inverse creation. PhotoniX, 2021, 2: 22
22 Jiang J, Chen M, Fan J A. Deep neural networks for the evaluation and design of photonic devices. Nat Rev Mater, 2021, 6: 679–700
23 Vanneste C, Sebbah P. Selective excitation of localized modes in active random media. Phys Rev Lett, 2001, 87: 183903
24 Cao H, Mosk A P, Rotter S. Shaping the propagation of light in complex media. Nat Phys, 2022, 18: 994–1007
25 Leonetti M, López C. Active subnanometer spectral control of a random laser. Appl Phys Lett, 2013, 102: 071105
26 Leonetti M, Conti C, Lopez C. Switching and amplification in disordered lasing resonators. Nat Commun, 2013, 4: 1740
27 Qiao Y, Peng Y, Zheng Y, et al. Adaptive pumping for spectral control of broadband second-harmonic generation. Opt Lett, 2018, 43: 787–790
28 Shi X, Song W, Liang N, et al. Manipulating laser modes in diffusive disordered systems by precisely designing the boundary of the local pump. Laser & Photonics Rev, 2023, 17: 2300188
29 Bachelard N, Andreasen J, Gigan S, et al. Taming random lasers through active spatial control of the pump. Phys Rev Lett, 2012, 109: 033903
30 Bachelard N, Gigan S, Noblin X, et al. Adaptive pumping for spectral control of random lasers. Nat Phys, 2014, 10: 426–431
31 Kumar B, Homri R, Priyanka R, et al. Localized modes revealed in random lasers. Optica, 2021, 8: 1033
32 Saxena D, Arnaudon A, Cipolato O, et al. Sensitivity and spectral control of network lasers. Nat Commun, 2022, 13: 6493
33 Turitsyn S K, Babin S A, Churkin D V, et al. Random distributed feedback fibre lasers. Phys Rep, 2014, 542: 133–193
34 Katoch S, Chauhan S S, Kumar V. A review on genetic algorithm: past, present, and future. Multimed Tools Appl, 2021, 80: 8091–8126
35 Hou C F, Tsui W A, Chou R J, et al. Speckle-free, angle-free, cavity-free white laser with a high color rendering index. ACS Appl Mater Interfaces, 2024, 16: 11489–11496